On the Cross-Section Structure of the Mitochondrial Cristae-Membrane as Revealed by X-Ray Diffraction

W. Müller-Klieser and W. Kreutz

Institut für Biophysik und Strahlenbiologie der Universität Freiburg

(Z. Naturforsch. **31 c**, 612–621 [1976]; received July 16, 1976)

Biomembranes, Mitochondria, X-Ray Diffraction, *Q*-Function, Electron Density Profile

Mitochondria were isolated using sorbitol and high buffer concentration in the medium. X-ray diffraction patterns arising from the mitochondrial cristae-membrane were recorded in the fully dried state and in two different states in humidity. The *Q*-function evaluation of these X-ray diffraction diagrams resulted in electron density cross-section profiles, which consist of two main peaks of opposite sign and one, respectively two, smaller peaks. The total thickness of the membrane amounts to 120 Å in the dry and 140 Å to 160 Å in the wet state. An interpretation of the cross-section profile is tentatively proposed.

Introduction

New evaluation methods of X-ray diffraction patterns of biomembranes, using the "*Q*-function method", allow the calculation of the cross-section profiles of the mitochondrial cristae-membrane. A conventional evaluation of the diagrams through a separate determination of the amplitudes and phases of diffraction peaks cannot be carried out because of the fact that only very small coherence regions, consisting of two membranes occur in this system. In addition, lattice distortions have to be considered.

The necessary experimental conditions were provided by developing a special preparation method in which the cristae-membrane could be stabilized over a long period of time, and also by employing fast recording position sensitive counter techniques.

Methods

Preparation

The fresh beef heart tissue was placed on ice, immediately post mortem and put into the medium in small cubes [1] as soon as possible. All preparative steps were carried out at 4 °C. The medium consists of 1 M sorbit, 50 mM Tris-HCl, 0.2 mM EDTA. The pH was adjusted to 7.4. After briefly mixing, the homogenate was pressed through a nylon net. Then 0.2 mM $MgCl_2$ were added to the obtained liquid. The pH was readjusted to 7.4. The mitochondria were then isolated by differential centrifugation [2].

Hypertonic conditions from 1 M sorbit and high buffer concentrations were applied in order to avoid undesired conformational changes [3, 4], and also to densely stack the cristae-membranes of the mitochondria. Sorbitol proved suitable to stabilize the membrane structure over a long period of time and also facilitated in largely conserving the membrane during drying. The process of washing out the substances dissolved in the medium led to the total desintegration of the membrane. This could be determined by X-ray diffraction and by electron microscopy. Sucrose was found to be unsuitable for desiccating since it often crystallized. Crystal reflexions were then super-imposed onto the X-ray scattering diagram of the membrane.

Requests for reprints should be sent to Prof. Dr. W. Kreutz, Institut für Biophysik und Strahlenbiologie, Universität Freiburg i. Br., Albertstraße 23, *D-7800 Freiburg i. Br.*

Biochemical control experiments

The pellet of the isolated mitochondria contained 12 μg phospholipid phosphorus/mg protein on the average; this was determined by a modified method of Bartlett [5]. The lipids were extracted by means of a modified Folch-method [6]. Protein was determined by the method of Lowry [7]. Protein composition of the preparation was checked with SDS-electrophoresis [8]. All the major proteins were present in the same proportions as in the analysis of Harmon *et al.* [9]. In the case of wet samples the succinate cytochrome c dehydrogenase activity was tested with the method of King [10]. The activity was largely conserved during X-ray exposure time. It was found to be 0.2 μmol cyt c/min/mg prot, which is comparable with values reported by Green *et al.* [11] for isolated mitochondria.

Electronmicroscopic control pictures

Electronmicroscopic thin sections of the mitochondria pellet served as controls for the conservation of the structure during the isolation method. They further showed that the beef heart mitochon-

dria contained at least ten times more cristae-membranes than outer membranes (Fig. 1 *). Thus, an X-ray diffraction experiment having scattering exclusively from stacked cristae-membranes is to be expected; the scattering of the outer membrane can be neglected.

X-ray diffraction techniques

X-ray diffraction diagrams of orientated dry and unorientated wet isolated mitochondria were recorded. To get orientated dry mitochondria the following procedure was applied. Isolated mitochondria obtained from 40 g beef heart tissue (corresponding to 10 to 12 mg mitochondria protein) were washed three times with 0.25 M sorbitol solution and spun down at $40.000 \times g$. When the supernatant was decanted a wet pellet of about 100 mg remained in the centrifuge tube. The mitochondria thus preorientated were put in the centrifuge tube into the desiccator. The further orientation was performed by drying the pellets for at least two days at room temperature. The sample was then taken out of the desiccator. The pellet was detached from the bottom of the tube as a thin dried plate of about 10 mm diameter and a thickness of about 0.5 mm. From this plate a stripe of about 1 mm width was cut with a razor blade. This stripe was softly pushed into a glass capillary and placed in the X-ray diffraction camera. The incident X-ray beam was directed both perpendicular and parallel to the plane of the thin stripe.

The wet state diagrams were produced in a specially constructed humidity chamber. The wet pellet was placed on a sample holder in the form of a drop, as similarly described by Finean *et al.* [12, 13]. The defined degrees of humidity were regulated by saturated salt solutions of $MgCl_2$, $K_2CO_3 \cdot 2\,H_2O$, $NaBr \cdot 2\,H_2O$, and KCl corresponding to 33.0%, 42.76%, 57.7%, 75.28%, and 84.26% humidity. The temperature in the humidity chamber was 4 °C during the measurements.

The X-ray diffraction diagrams were recorded with a Kratky-camera as well as with a Kiessig-camera and with a camera according to Schnabel *et al.* [14]. In the case of the Kratky-camera the line collimation system was changed into a point-like collimation by introduction additional vertical slits. The registration was performed by film and by a position sensitive proportional counter. The counter and the electronic measuring arrangement (conventional nuclear electronic) were constructed by J. Fritz and M. Henne according to a description by Gabriel and Dupont [15]. The resolution was improved from 150 μm to 80 – 120 μm, depending on the counter chamber used. During measurement the counter was operated by a gas-flow method. Xenon, with 10% methane as a quenching additive, was used as the tube gas. Voltage at the detector was 1200 V to 1300 V, also depending on the chamber used.

Results

The diagrams of cristae-membranes in the dry state (Fig. 2 a) consist of six or seven broad diffraction orders of a stacking period in the range of 260 Å to 280 Å (resolution about 30 Å) and an additional sharp ring at about 42 Å, often showing slightly hexagonal orientation. The reflexion can be clearly separated from the broad stacking reflexions by its different orientation as well as by its narrow intensity profile (Fig. 2 a). In very rare cases the ring corresponds to a 50 Å-Bragg spacing. It then shows a broad profile and is very weak in its intensity.

The additional occurrence of a ring-shaped reflexion may be interpreted as a partial desintegration within the membrane, where lipoproteins or lipids crystallize out of the membrane structure. This reflexions could be routinely observed below a humidity degree of 33%. Furthermore, it occurs if the sample is warmed to room temperature, or if mitochondria are kept under unaerobic conditions. The occasional hexagonal orientation of the reflexion cannot be understood at the moment.

If the direction of the incident beam is chosen perpendicular to the plane of the dried sample, a sharp intensive ring at 42 Å, a weak sharp ring at 48 Å, and very weak broad ring at about 100 Å appear (Fig. 2 b).

In the range between 33% and 75% humidity only a series of broad stacking interferences were recorded. The first order reflexion corresponds to a Bragg spacing of 360 Å (see Fig. 3 b).

The absence of additional reflexions which occur below 33% humidity was taken as a criterion for the membrane being structurally intact.

Above 75% humidity only continuous scattering curves were observed (see Fig. 3 c).

Inspite of the apparent partial denaturation below 33% humidity the scattering diagrams of dry cristae-membranes were evaluated also, in order to investigate the influence of the partial desintegra-

* Figs 1 and 2 see Plate on page 614 a.

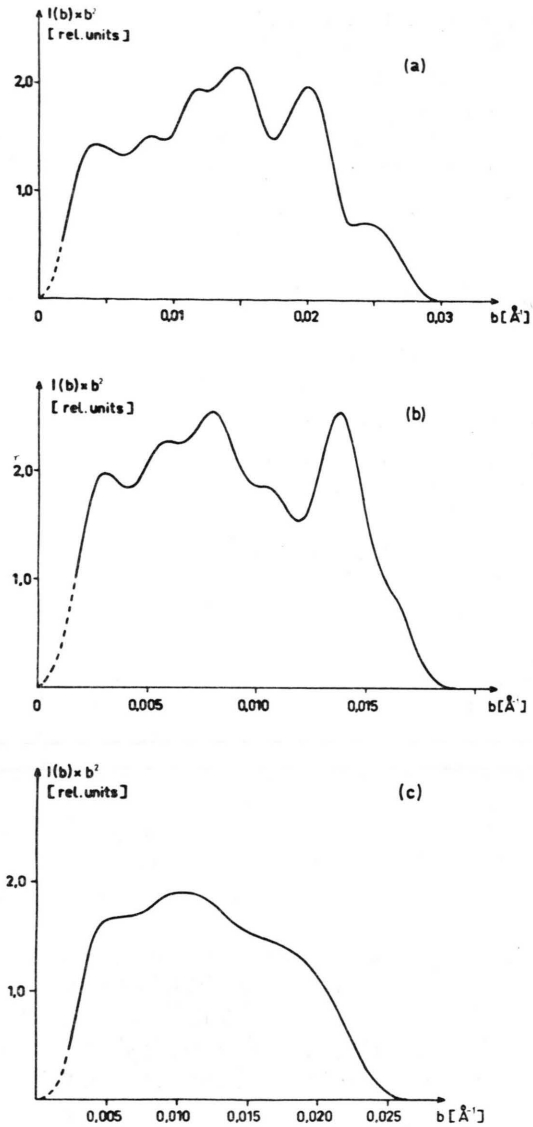

Fig. 3. Intensity diagram after elimination of the Lorentz-factor and after Gauss-elimination of the "O-peak". (- - - -) Gauss extrapolation of the first order peak. a. Mitochondria at <30% humidity ("dry"); b. mitochondria at 33% humidity ("wet") (corresponding diagrams were observed at 42.76%, 57.7%, and 75.28% humididy); c.mitochondria at 100% humidity.

tion onto the membrane structure in comparison with the two other types of scattering diagrams.

The densitometer tracings of the film diagrams were recorded with a double beam densitometer of Joyce, Loebl a. Co., model MK III C. From the intensity curves thus obtained, as well as from the intensity curves recorded by the position sensitive counter, the Lorentz-factor was eliminated for further evaluation. These curves are shown in Fig. 3 a – c.

The elimination of the "O-peak"-contribution in the diagrams was performed by a Gaussian extrapolation of the first order intensity peak.

For eliminating the background scattering, *i. e.* scattering of non-lamellar components, the equatorial scattering was subtraced from the meridional scattering which was done with patterns of well orientated dry samples. A comparison of these evaluations with those neglecting the background scattering, however, showed that the same profiles are obtained in principle. The background scattering slightly influences only the relative peak-heights; therefore, the evaluation of diffraction patterns in the wet state was done without eliminating the background scattering.

Calculation of the electron density profiles

The electron density profiles were calculated by means of the so-called Q-function method according to Hosemann and Bagchi [16]. This method was first applied to biological objects by Kreutz [17, 18] and later used by Pape [19] and Lesslauer *et al.* [20]. The Q-function is the Fourier-transform of the measured intensity distribution. In the case of finite crystals a periodic decreasing function is obtained which decreases the faster the smaller the crystal is. For stacks of biological membranes the periodicity corresponds to the length of a double membrane or to a double membrane with an interspace respectively. It is possible to separate the so-called Q_0-function from the Q-function by continuous "mirror symmetrical subtraction" as described by Kreutz [17]. The Q_0-function represents the convolution square of the electron density distribution of a double membrane, *i. e.* the lattice cell (unit cell). Based on the assumption of a centro-symmetrical density distribution of the lattice cell, Hosemann [16] showed that the deconvolution of the Q_0-function can be solved uniquely except for one sign. Pape [19] developed the corresponding calculation procedure.

Biological membranes principally form closed units, for instance vesicles, tubes, membrane-like invaginations etc. In stacking such systems the projection of the electron density profile onto the stacking axis will always represent a series of images and mirror images, *i. e.* the electron density projection of the double membrane possess a centre of symmetry. This also applies to stacks of whole mito-

Fig. 1. Electronmicroscopic picture of isolated $KMnO_4$ stained mitochondria (preparation control picture), K. Goebel, J. Fritz.

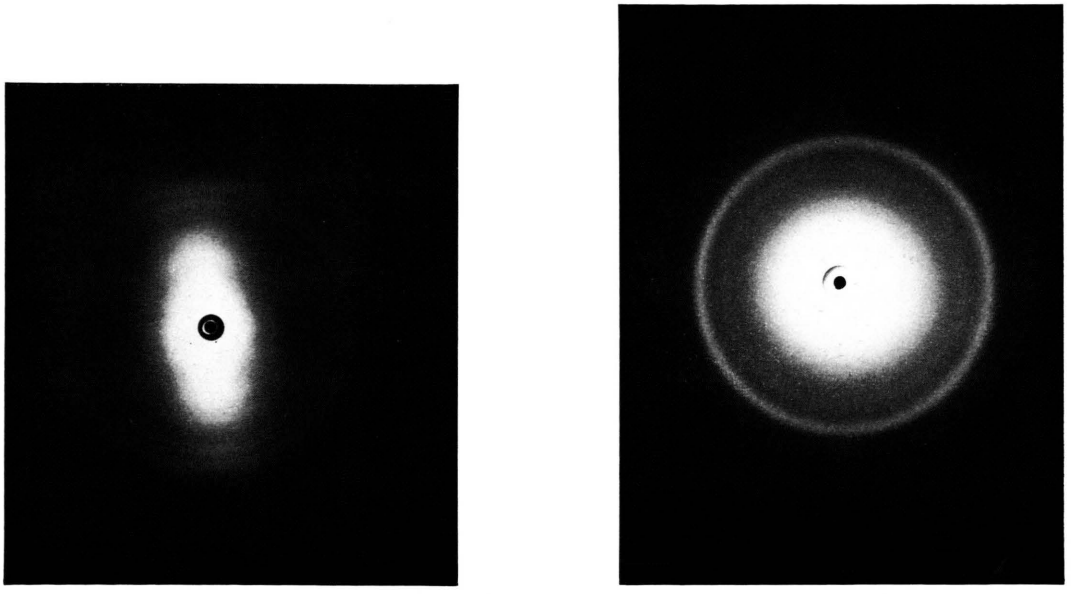

Fig. 2. X-ray pattern (Kiessig-Camera) of desiccator dry orientated mitochondria (humidity $<30\%$). a. Incident X-ray beam parallel to the membrane plane; b. incident X-ray beam perpendicular to the membrane plane. Distance sample to film 50 cm, magnification 1:1.

chondria with respect to the cristae-membrane (Fig. 4).

However, the isolation of Q_0, described above, is not possible because an exact stacking is not to be expected due to the intrinsic arrangement of the

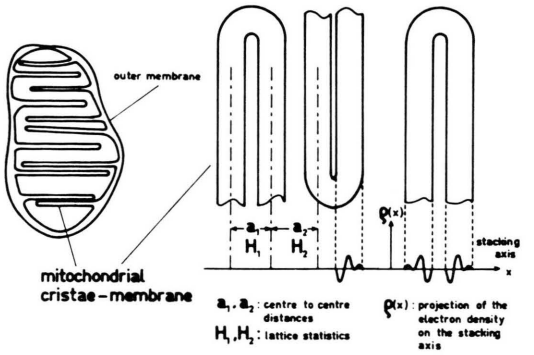

Fig. 4. Schematic representation of the parameters determining the paracrystalline state of the cristae stacks.

cristae-membranes within the mitochondria. It is more likely that cristae-double membranes form small paracrystalline regions and that there are even lattice distortions within the configuration of the double membrane. For the mathematical treatment of such a paracrystal, an arrangement of membranes with two different lattice statistics H_1 and H_2, has to be considered, as shown in Fig. 4. The Q-function for this case is given by the equation [21];

$$\begin{aligned} Q(x) &= N\, Q_{\mathrm{m},0} * \delta(x-0) \\ &+ (N-1)\,0.5\,[Q_{\mathrm{m},2} * H_1(x-a_1) + Q_{\mathrm{m},1} * H_2(x-a_2)] \\ &+ (N-2)\,Q_{\mathrm{m},0} * H_1(x-a_1) * H_2(x-a_2) + \ldots \\ &\quad \ldots + (N-(2k+1))\,0.5\,[Q_{\mathrm{m},2} * H_{1,k} \\ &\qquad * H_{2,k} H_1(x-a_1) + \\ &+ Q_{\mathrm{m},1} * H_{1,k} * H_{2,k} * H_2(x-a_2)] + \qquad (1) \\ &+ (N-2k)\,Q_{\mathrm{m},0} * H_{1,k} * H_{2,k} + \ldots \end{aligned}$$

where

$$\delta(x-0) = \infty \quad \text{for } x=0$$
$$0 \quad \text{for } x \neq 0$$
$$\text{with } \int_{-\infty}^{+\infty} f(x)\,\delta(x)\,\mathrm{d}x = f(0)$$

$Q_{\mathrm{m},0} = \tilde{\tilde{\varrho}}_{\mathrm{m}}$; $\varrho_{\mathrm{m}} = \varrho_{\mathrm{m}}(x)$ = electron density profile of a single membrane;

$Q_{\mathrm{m},1} = \varrho_{\mathrm{m}} * \varrho_{\mathrm{m}}$;

$Q_{\mathrm{m},2} = \varrho_{-\mathrm{m}} * \varrho_{-\mathrm{m}}$; $\varrho_{-\mathrm{m}}(x) = \varrho_{\mathrm{m}}(-x)$;

$\tilde{\tilde{\varrho}}_{\mathrm{m}} = \int_{-\infty}^{+\infty} \varrho_{\mathrm{m}}(y)\,\varrho_{\mathrm{m}}(y-x)\,\mathrm{d}y$ = convolution square of ϱ_{m};

$\varrho_{\mathrm{m}} * \varrho_{\mathrm{m}} = \int_{-\infty}^{+\infty} \varrho_{\mathrm{m}}(y)\,\varrho_{\mathrm{m}}(x-y)\,\mathrm{d}y$ = convolution product of ϱ_{m};

N = number of stacked membranes;

a_1, a_2 = centre to centre distance of a membrane to its next neighbours;

H_1, H_2 = lattice statistics corresponding to a_1 and a_2 (see also Fig. 4);

$H_{1,k}$ = H_1, $(k-1)$-times convoluted with itself.

Formula (1) is valid only for the case of a sum of equally large paracrystals of N-membranes. However, it must be assumed that the intensity distribution is formed by incoherent superposition of the scattering of paracrystalline regions differing in size. Since these variously extensive coherent regions occur with a diverse frequency in the object, the terms in the Eqn (1) have to be supplement with weight factors.

In the case of the cristae-membranes, which, compared with other membranes, such as myelin or disc membranes are poorly stacked originally, the first three terms of Eqn (1) already suffice for the analytical representation of the experimental Q-function, since it practically decreases to zero after one "long-period", *i. e.* the thickness of one double membrane plus interspace. Thus, the scattering of the single membrane, Eqn (2), and of both combinations of a double membrane, Eqns (3) and (4) contribute to the Q-function, as shown in Fig. 5.

$$Q^*_{\mathrm{m},0} = \tilde{\tilde{\varrho}}_{\mathrm{m}}. \qquad (2)$$

$$Q^*_{\mathrm{m},1} = 2\,\tilde{\tilde{\varrho}}_{\mathrm{m}} + \varrho_{-\mathrm{m}} * \varrho_{-\mathrm{m}} * H_1(x-a_1). \qquad (3)$$

$$Q^*_{\mathrm{m},2} = 2\,\tilde{\tilde{\varrho}}_{\mathrm{m}} + \varrho_{\mathrm{m}} * \varrho_{\mathrm{m}} * H_2(x-a_2). \qquad (4)$$

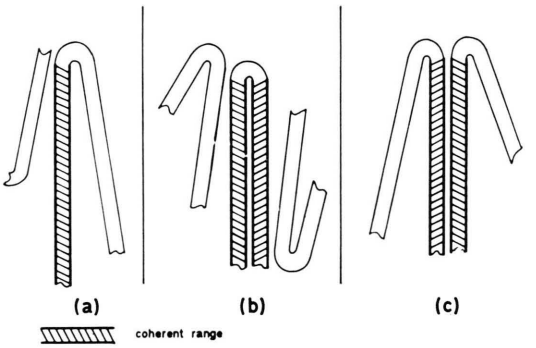

Fig. 5. Membrane combinations contributing to the Q-function represented by Eqn (5). a. Single membranes represented by Eqn (2); b. double membranes corresponding to Eqn (3) (inside-inside-coupling); c. double membranes corresponding to Eqn (4) (outside-outside-coupling).

The total Q-function is then given by the sum of the contributions (2), (3), and (4), whereby each contribution must be multiplied with a weight factor G_i:

$$Q = G_0 Q^*_{m,0} + G_1 Q^*_{m,1} + G_2 Q^*_{m,2} . \quad (5)$$

For the further calculation procedure the terms are comprised in the following way:

$$Q = G \overset{2}{\varrho}_m * \delta(x-0) + G_1 \varrho_{-m} * \varrho_{-m} * H_1(x-a_1) + G_2 \varrho_m * \varrho_m * H_2(x-a_2), \quad (6)$$

whereby

$$G = G_0 + 2G_1 + 2G_2 .$$

It follows from Eqn (6) that the choice of the weight factors is restricted by the condition:

$$G \geqq 2G_1 + 2G_2 . \quad (7)$$

For the analytical representation of the experimental Q-function according to Eqn (6), two calculation procedures are applied.

In a procedure developed by Pape [22] the electron density profile is represented by a sum of Gaussians using an initial set of parameters A_k, x_k, c,

$$\varrho_m = \sum_k A_k \exp\left(-c(x-x_k)^2\right) . \quad (8)$$

The Q-function is calculated according to Eqn (6) using Gaussians with variable half-widths for the two statistics H_1 and H_2. All parameters are varied until the synthesized Q-function is sufficiently fitted to the experimental Q-function. To attain this, a least squares refinement technique according to Marquardt [23] is applied. For the fit 6 Gaussians were needed to describe the electron density distribution.

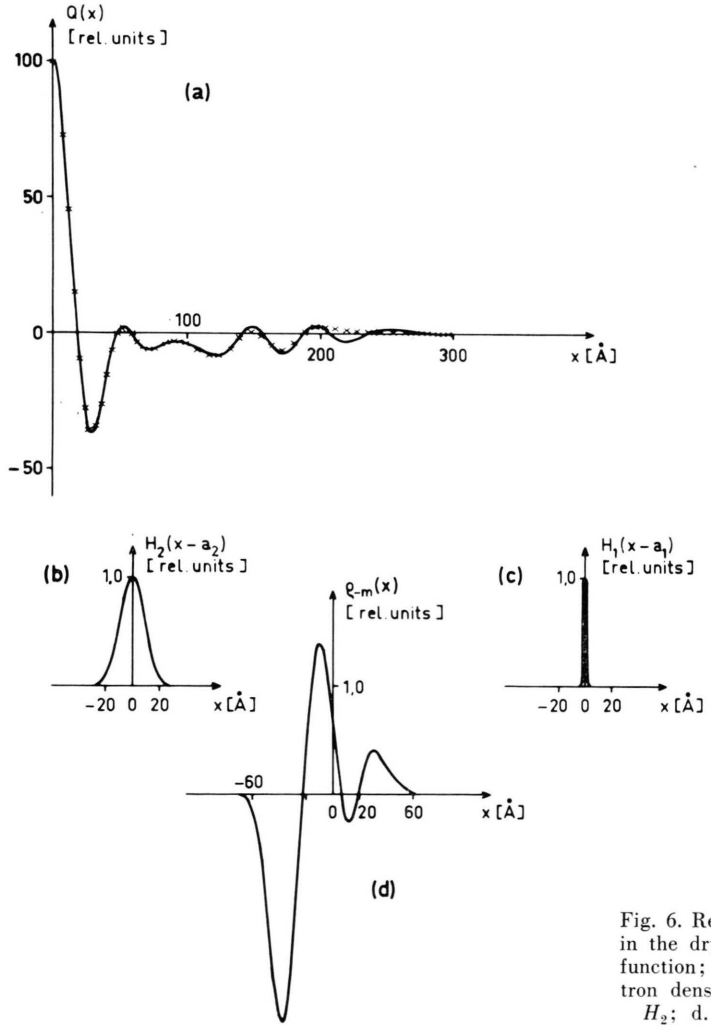

Fig. 6. Results of the Q-function evaluation of mitochondria in the dry state: a) Q-functions: ——— experimental Q-function; +++ Q-function calculated from the found electron density; b. c. applied lattice statistics functions H_1, H_2; d. electron density profile of one cristae-membrane.

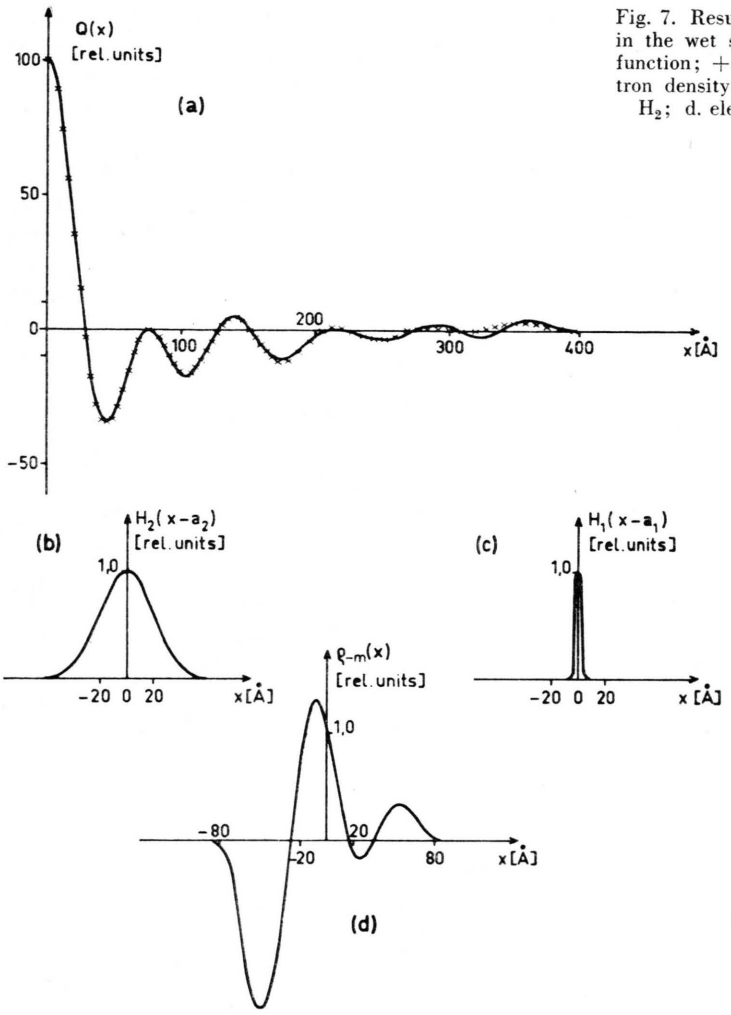

Fig. 7. Results of the Q-function evaluation of mitochondria in the wet state: a. Q-functions: ——— experimental Q-function; +++ Q-function calculated from the found electron density; b. c. applied lattice statistics functions H_1, H_2; d. electron density profile of one cristae-membrane.

(The fit could not be achieved with less Gaussians and could not be improved by chosing more than 6 Gaussians.)

The other procedure has been described by Welte [24]. In this case a fourier analytical representation of the electron density is chosen. The Q-function is again evaluated under consideration of two lattice statistics (Gaussians H_1 and H_2). Hereby, the Marquardt technique fits the Fourier-integrals of the theoretical Q-function to the Fourier-integrals over the measured Q-function.

Both procedures result in similar electron density profiles for the cristae-membranes in the dry state ($<33\%$ humidity) shown in Fig. 6, and in the wet state ($33-75\%$ humidity), demonstrated in Fig. 7. The profile of cristae-membranes in the 100% humidity state (Fig. 8) was calculated in a different way in order to check the number of possible solutions for the profile $\varrho_m(x)$ as will be discussed in the next chapter.

Evaluation of the number of solutions for $\varrho_m(x)$

As already mentioned above, according to Hosemann [16], the deconvolution of the Q_0-function of a centro-symmetrical lattice cell $\varrho_0(x)$, which is not statistically distorted, results in a unique solution for $\varrho_m(x)$ in the case the Q_0-function is represented only by one convolution square and by one convolution product of $\varrho_m(x)$:

$$Q_0(x) = \tilde{\tilde{\varrho}}_0(x) = 2\,\tilde{\tilde{\varrho}}_m + \varrho_m * \varrho_m * \delta(x-a) \quad (9)$$

$(x>0)$

$\varrho_0(x)$ = profile of the double membranes.

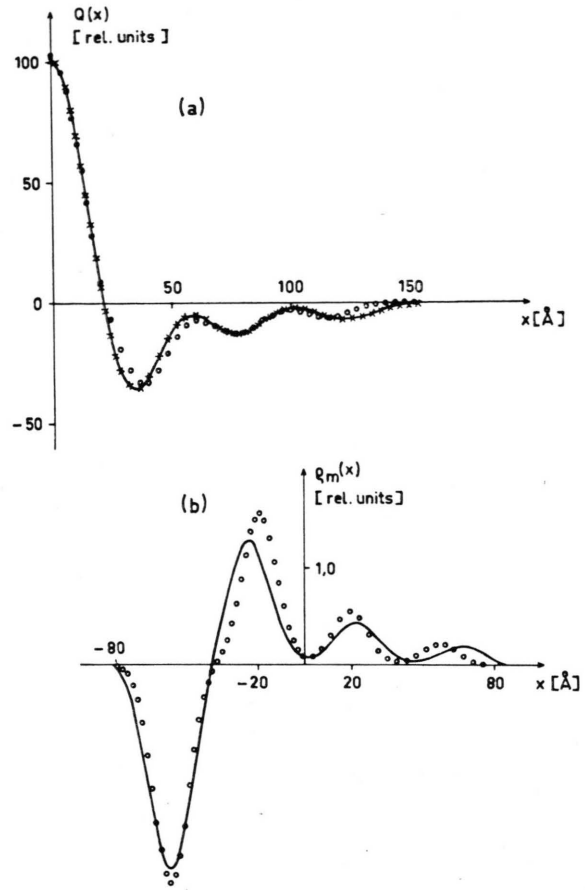

Fig. 8. a. Q-function of mitochondria at 100% humidity. ——— experimental Q-function; ○○○ Q-function represented by a sum of equidistant Gaussians; ××× Q-function represented by a sum of none-equidistant Gaussians. b. electron density profile of a single cristae-membrane ——— profile represented by a sum of none-equidistant Gaussians; ○○○ profile represented by a sum of equidistant Gaussians.

However, in the analytical representation of the experimental Q-function according to Eqn (6) the superposition of the Q_0-functions of two distorted lattice cells, namely $Q_{m,1}$ and $Q_{m,2}$, and in addition the convolution square $\tilde{\varrho}_m^2$ have to be taken into account. Due to these superpositions and due to the lattice statistics $H_1(x)$ and $H_2(x)$ several solutions for the profile ϱ_m may exist.

The analytical representation of the Q-function according to Eqn (6) always leads to the same profile type, though it was performed by two different calculation procedures for three different Q-functions (three hydration states). Many attempts to find other solutions for ϱ_m by changing the parameters of Eqn (6) or introduction further terms of Eqn (1) failed. In order to get further approach to the number of possible solutions a semi-analytical procedure was applied, which is described in the following.

In the case of cristae-membranes it can be shown that the part of Eqn (6) with the two convolution products decreases systematically with increasing hydration. If the atmosphere in the humidity chamber reaches 100% relative humidity the Q-function consists only of the convolution square of one single membrane, as demonstrated in Fig. 8a. This means that the scattering intensity of one single membrane is recorded. The corresponding intensity curve is depicted in Fig. 3 c. For evaluating the convolution root of the Q-function in Fig. 8 a a procedure was used which was developed by Weick [25, 26]. Thereby the convolution square of ϱ_m is approximated by equidistant Gaussians of equal half-widths. The electron density profile then also consists of equidistant Gaussians with equal half-widths, the amplitudes A_i of which are correlated with the Gaussian amplitudes G_j of the convolution square by the following equation:

$$G_j = \sum_{j=1}^{N-j+1} A_i A_{i+j-1}, \qquad (10)$$

where $j = 1 \ldots N$;

N = number of Gaussians in the convolution square;

G_j = amplitudes of Gaussians in the convolution square;

A_j = amplitudes of Gaussians in the electron density profile.

In the case of the hydrated cristae-membrane the convolution square $\tilde{\varrho}_m^2$ of Fig. 8 a can be totally approximated by only four Gaussians. The system of four equations resulting from Eq. (8) is solved semi-analytically. Within the scope of accuracy of the measurement this procedure also yields only one solution and its mirror image which is shown in Fig. 8 b. After that the profile is fitted to the experimental Q-function giving up the restriction of the equidistance for the Gaussians. Thereby the profile does not change essentially as can be seen in Fig. 8 b.

Except for the negligibly small additional positive peak, the profile in Fig. 8 b shows all essential features of the profiles evaluated to describe the Q-

function of dry and wet cristae-membranes containing convolution products.

If strong lattice distortions occur in small coherence regions, as in the case of stacks of "dry" and "wet" cristae-membranes, the inner part of the corresponding Q-functions is mainly formed by $\tilde{\tilde{\varrho}}_m$, the convolution square of the single membrane. Thus, it seems reasonable, that the deconvolution procedures in the three cases discussed above, result in the same profile types.

Comparison with previous investigations

In 1960 Worthington [27] suggested a simple step-model profile for the electron density cross-section of the cristae-membrane in order to explain the X-ray intensity distribution, he obtained from insect flight muscles. His results were too rough to make a meanigful comparison to the profiles derived here.

Thompson *et al.* [28, 29] published X-ray diffraction diagrams of isolated inner and outer membranes of rat liver mitochondria, without, however, evaluating the intensity curves. The Bragg spacings given by Thompson for the dehydrated state are 90 Å, 62 Å, 49 Å. The stacking period found in our investigations, varies between 260 Å and 280 Å in the dry state. The third, fourth, and fifth order of our system, therefore, corresponds with the spacings given by Thompson. The first two orders are rather difficult to measure because of the strong continuous scattering at low angles. In the wet state the strongest orders measured were found at 120 Å and at 79 Å, *i. e.* third and fifth order reflexions. These two reflexions were also found by Thompson, whereas a 57 Å-reflexion could not be detected.

Discussion of the profiles

The evaluation of the X-ray scattering curves renders the same profile type for the cristae-membrane in three hydration states. The charateristic features of the profile are the two main peaks of opposite sign and one, respectively two, smaller peaks. As can be shown by model calculations [24] the slight uniform increase of the width of the Gaussians may partially be due to corrugations of the membrane in the humid state causing a broadening and "smearing" effect of the profiles. This may also explain the fact that electron density details (*e. g.* peaks of lipid polar headgroups) are not apparent in the profiles. In addition, dehydration effects on the membrane structure may also be responsible for the slight deviations between the three profiles.

An essential view-point for the interpretation of the two profiles given in Fig.9 a and 9 b (image and mirror image) is, that in one case a strong negative electron density peak is positioned at one side of the membrane, in the other case in the center of the membrane. Therefore, in profile 9 a lipids should be dominantly arranged at one side of the membrane, mainly forming a monolayer, whereas in profile 9 b a central lipid bilayer should exist. The proteins in profile 9 a would form two definite layers, a

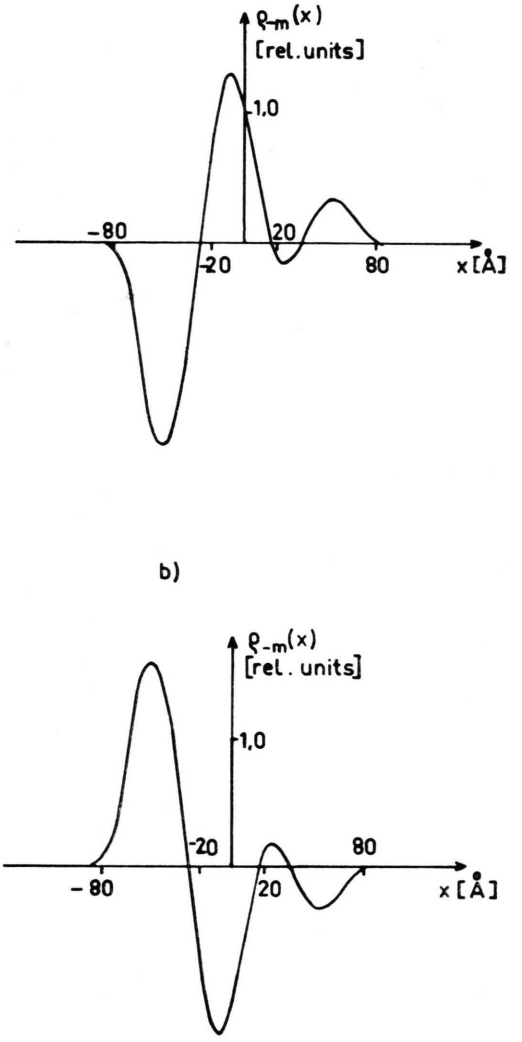

Fig. 9. Image (a) and mirror-image (b) of the electron density profile (the two solutions of the Q-function).

central intrinsic protein layer, and an outer extrinsic protein layer. In profile 9 b, however, no appreciable amount of protein could exist in the center of the membrane but should be asymmetrically arranged at both sides of the bilayer.

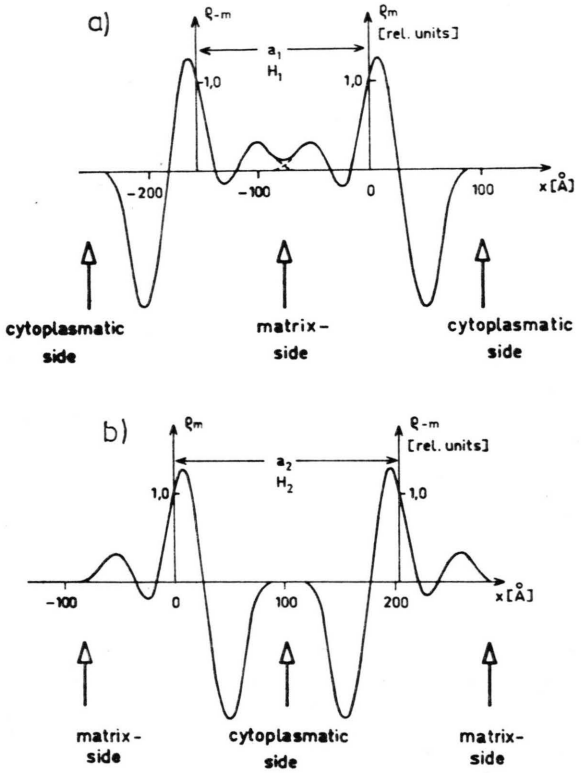

Fig. 10. "Sidedness" of the membrane combinations for the solution of Fig. 9 a. a. According to $Q_{m,1}$ (Eqn (3)); b. according to $Q_{m,2}$ (Eqn (4)).

Biochemical localization experiments [9] indicate that the proteins are situated either in the inner part of the membrane as intrinsic proteins (55%) or they are – apart from cytochrome c ($\cong 1\%$) – located at the matrix-side of the membrane as extrinsic proteins ($\cong 44\%$). This corresponds with many electron microscopic studies (*e. g.* Fernandez-Moran *et al.* [30]) which imply that the proteins form two layers, one "continuous" layer and another forming the characteristic particles. In addition it was shown by Green *et al.* [31] that there is evidence for the lipids to be mainly arranged at the cytoplasmatic membrane-side.

These findings favour profile 9 a with a "sideness" as it is shown in Fig. 10 a and 10 b, where the two coherence regions formed by the two membrane combinations (see Fig. 5 and Eqns (3) and (4)) are depicted. However, a final decision whether profile 9 a or 9 b is the right solution for the membrane's profile cannot be made on the basis of experimental data presently available.

We are very indebted to Dr. E. H. Pape for helpful discussions and advice in the computation procedures. Many thanks also to Mr. R. Mull for his assistance in preparing this manuscript. The deconvolution procedures were calculated at the Computer Centre of the University of Freiburg.

[1] C. Fourcade and J. Decotes, Triangel **13**, 173 [1975].
[2] Y. Hatefi, P. Jurtschuk, and A. G. Haavik, Arch. Biochem. Biophys. **94**, 148 [961].
[3] J. T. Penniston, R. A. Harris, J. Asai, and D. E. Green, Proc. Nat. Acad. Sci. U.S. **59**, 624 [1968].
[4] R. A. Harris, J. T. Penniston, J. Asai, and D. E. Green, Proc. Nat. Acad. Sci. U.S. **59**, 830 [1968].
[5] Bartlett, Techniques of Lipidology, 1959.
[6] J. L. Holtzmann and J. R. Gilette, J. Biol. Chem. **243**, 3020 [1968].
[7] O. H. Lowry, N. J. Rosebrough, N. J. Farr, and R. J. Randall, J. Biol. Chem. **193**, 265 [1951].
[8] K. Weber and M. Osborn, J. Biol. Chem. **244**, 4406 [1969].
[9] H. J. Harmon, J. D. Hall, and F. L. Crane, Biochim. Biophys. Acta **344**, 119 [1974].
[10] T. E. King, J. Biol. Chem. **238**, 37 [1963].
[11] D. E. Green, R. L. Lester, and D. M. Ziegler, Biochim. Biophys. Acta **23**, 516 [1957].
[12] J. B. Finean, R. Coleman, and W. A. Green, Ann. Rev. N. Y. Acad. Sci. **137**, 414 [1966].
[13] J. B. Finean, R. Coleman, W. A. Green, and A. R. Limbrick, J. Cell. Sci. **1**, 287 [1966].
[14] E. Schnabel, H. Röde, and R. Hosemann, J. Appl. Phys. **43**, 3237 [1972].
[15] A. Gabriel and Y. Dupont, Rev. Sci. Instrum. **43**, 1600 [1972].
[16] R. Hosemann and S. N. Bagchi, Direct Analysis of Diffraction by Matter, North Holland Publ. Co., Amsterdam 1962.
[17] W. Kreutz, Habilitationsschrift D 83, Technische Universität Berlin 1968.
[18] W. Kreutz, Advan. Bot. Res. **3**, 53 [1970].
[19] E. H. Pape, Biophys. J. **14**, 284 [1974].
[20] W. Lesslauer, J. Cain, and J. K. Blaisie, Biochim. Biophys. Acta **241**, 547 [1971].
[21] W. Kreutz and E. H. Pape, Sumer Institute on the Physics of Biological Membranes (K. Clobow, ed.), Simon Fraser University, Vancouver, B.C., Canada, 1975.
[22] E. H. Pape, K. Klott, and W. Kreutz, in preparation.
[23] D. W. Marquardt, J. Soc. Appl. Math. **11**, 431 [1963].
[24] W. Welte and W. Kreutz, to be published.
[25] D. Weick, R. Hosemann, E. H. Pape, and W. Menke, Colloid & Polymer Sci. **252**, 819 [1974].
[26] E. H. Pape, W. Menke, D. Weick, and R. Hosemann, Biophys. J. **14**, 221 [1974].
[27] C. R. Worthington, J. Mol. Biol. **2**, 327 [1960].
[28] J. E. Thompson, R. Coleman, and J. B. Finean, Biochim. Biophys. Acta **135**, 1074 [1967].

[29] J. E. Thompson, R. Coleman, and J. B. Finean, Biochim. Biophys. Acta **150,** 405 [1968].
[30] H. Fernandez-Moran, T. Oda, P. V. Blair, and D. E. Green, J. Cell. Biol. **22,** 63 [1964].
[31] D. E. Green, D. W. Allmann, E. Bachmann, H. Baum, K. Kopaczyk, E. F. Korman, S. Lipton, D. MacLennan, D. G. MacConnell, J. F. Perdue, J. S. Rieske, and A. Tzagoloff, Arch. Biochem. Biophys. **119,** 312 [1967].